Designing Helium-Filled Aerostats Applying Scaling Procedure, Mini-Models CANDY and Fly-Tests on SKYLAB

Jan Holnicki-Szulc, Lech Knap, Andrzej Świercz, Grzegorz Mikułowski, and Cezary Graczykowski

1 Introduction

Airships and balloons were the first men-built flying vehicles. Although their initial development has been intensive, during the last century, they have been to a large extend replaced by aircrafts. However, recent technological developments, such as production of advanced ultra-light helium-tight materials, have caused a renewed interest in aerostats. Currently, produced lightweight airships (Fig. 1a) have an ability to carry out long-term and low-energy missions at much lower costs than aircrafts [1]. They successfully fulfil various civil and military tasks, e.g. provide communication (4G/5G technology) in hardly reachable areas and serve as reconnaissance and surveillance systems or research pseudo-satellites [2]. Stratospheric airships provide local connectivity in areas of natural disasters or areas with a low level of ground infrastructure [3]. Moreover, the total costs for cargo transport or for exploration of stratosphere, mesosphere and even space observation using airships are much lower than in case of using airplanes or standard satellites [4, 5].

J. Holnicki-Szulc · A. Świercz · G. Mikułowski · C. Graczykowski (✉)
Institute of Fundamental Technological Research, Polish Academy of Sciences, Warsaw, Poland
e-mail: cgraczyk@ippt.pan.pl

J. Holnicki-Szulc
e-mail: holnicki@ippt.pan.pl

A. Świercz
e-mail: aswiercz@ippt.pan.pl

G. Mikułowski
e-mail: gmikulow@ippt.pan.pl

L. Knap
Institute of Vehicles and Construction Machinery, Warsaw University of Technology, Warsaw, Poland
e-mail: lech.knap@pw.edu.pl

© The Author(s), under exclusive license to Springer Nature Singapore Pte Ltd. 2023

D. Shukla (ed.), *Lighter Than Air Systems*, Lecture Notes in Mechanical Engineering,
https://doi.org/10.1007/978-981-19-6049-9_13

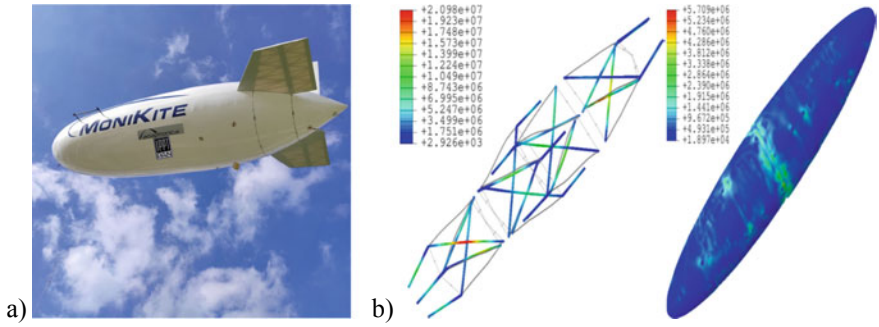

Fig. 1 **a** Classic tethered aerostat with well-designed aerodynamics developed by authors and **b** modelled aerostat-SDT with supporting tensegrity structure

Aerostat-SDT (aerostat with Self-Deployable Tensegrity) [6, 7] is an aerostat filled with gas from the storage tank with compressed helium (and storage tank with air used for ballonets) with well designed, aerodynamic shape and internal self-adaptive tensegrity-based supporting structure (Fig. 1b). Its shape can be automatically modified (increasing total volume, together with preserving aerodynamic properties and minimizing wind drift) during climbing up, from the starting level H_1 (lifted by an aircraft, rocket or by a traditional and hot-air balloon—Fig. 2), to the final altitude H_2. At altitude H_2, after monitoring mission is completed, the descent phase can be started utilizing the self-adaptive shape control of the aerostat.

The problem of optimal Aerostat-SDT design, to perform (with minimal cost of helium and energy consumption) determined mission (timing, the levels H_1 and H_2 and the payload to be lifted) with planned vertical mobility can be solved via numerical simulations, but the corresponding experimental verification can be complicated and costly. Especially, testing of V-Mobility (i.e. vertical mobility) dynamics via control of release valves for helium and ballasting air can be important.

Fig. 2 **a** Balloon SKYLAB and **b** mini-model CANDY with two ballonets

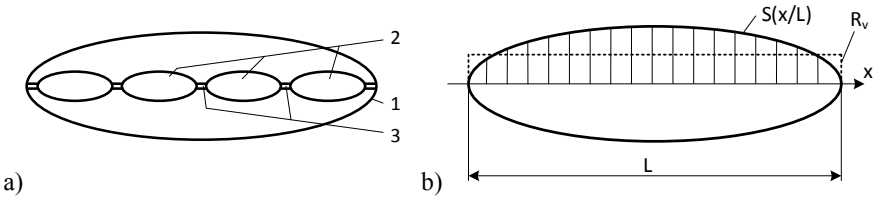

Fig. 3 **a** Mini-model aero-SDT—option with adaptive tendons: 1—external rigid shell, 2—internal softshell, 3—adaptive tendons and **b** a scheme of the scaled aerostat

2 Testing V-Mobility Via Mini-Models CANDY

V-Mobility control via gas release (ballasting air from ballonets for climbing up and helium from the other ballonet for descending) and the shape adaptation (morphing composed of the volume and aerodynamics modifications) can be tested taking advantage of a traditional, hot-air balloon (see Fig. 2a), so-called SKYLAB, towing up mini-model CANDY (see Fig. 2b), with the total mass known and also with monitored towing force F in the towing rope. Additionally, by measurements of physical parameters (temperature, external and internal pressures in the CANDY and its ballonets and mass of released gases) the buoyancy force can be determined and dynamics of vertical movement calculated.

In order to make manufacturing of mini-models easier, instead of the internal tensegrity structure, let us consider another option for controlling of the morphing process (cf. Fig. 3), so-called Aero-SDT (Self-Deployment and adaptive Tendons). The impermeable CANDY shell (2) with tight, light and very low deformable second layer (1) but equipped with adaptive strings with controllable length (3) allow effective tuning of the CANDY volume, together with the aerodynamic shape (superposed morphing).

3 Volume Measurement by Optical Technique

One of the objectives in the conducted research is to propose a procedure for determination of the physical volume of the inflated objects. Since the considered laboratory objects are fabricated in small series or even as single pieces, the repetitiveness of the production process always needs to be confirmed. Moreover, a fact is that the exact geometry of the object may rely on the changes in environmental parameters, i.e. temperature and pressure. Therefore, it becomes important to propose an adequate measuring method that is capable of identifying the modifications of the object. The measurement may be conducted by means of utilization of non-contact and optical methods, e.g. photogrammetry.

The chosen measurement method is stereo photogrammetry based on triangulation principle. Main hardware part are two cameras positioned in a precisely defined

mutual position. The cameras set-up is capable to record double picture of the object that is covered with dedicated markers, in order to reconstruct the surface in 3D. Due to large scale of the measured object, a strategy of multistage photography is chosen. The multistage approach assumes recording consecutive fragments of the whole structure in order to reach the complete picture. The following step is post-processing of the recorded pictures and data analysis.

The post-processing stage consists of 3D points determination and defining the surface of the object. Within data analysis stage, a volume of the object is calculated. In the case of the ellipsoidal shape objects, the proposed calculation method may be called "truncated cone integration". The object is divided into cones with a defined spatial step, and the object's volume is calculated as a numerical integral.

The measuring task was to determine a volume of inflated structure depicted in Fig. 4a, which also presents the triangulation set-up with two cameras of 4-megapixel resolution. The object is covered with dedicated optical markers positioned on the surface in a random manner (Fig. 4b). An exemplary geometry and volume identification during the post-processing stage is depicted in Fig. 5.

Accuracy of the method is dependent on several factors that need to be taken under consideration at each stage of the process. At the stage of the picture taking, the accuracy is relevant to the number of optical markers deposited on the identified surface. At the second stage—volume calculation—the number of elementary truncated cones taken for analysis is important factor influencing the final accuracy. Both the measurements carried out, and results obtained revealed high adequacy of the proposed approach.

a)  b) 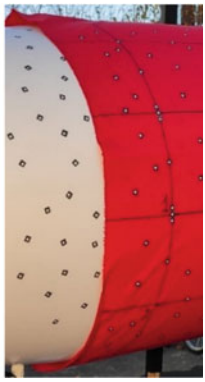

Fig. 4 Experimental set-up: **a** experimental object and set-up of cameras and **b** optical markers on the surface

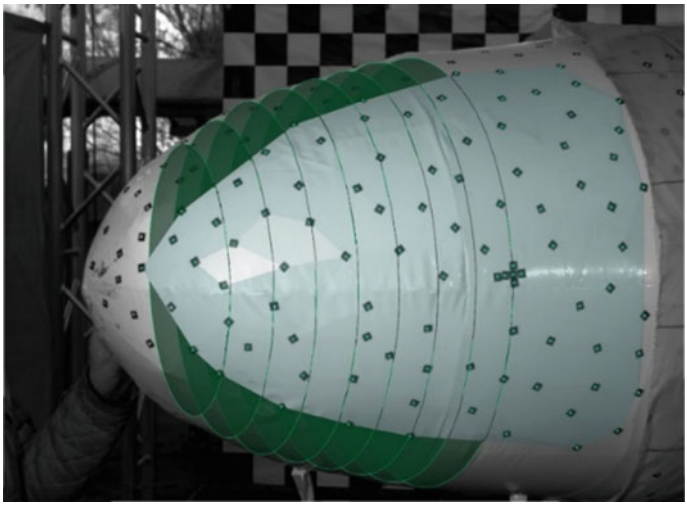

Fig. 5 Example of the left camera picture with post-processing overlayed

4 The Scaling Procedure

Assume the optimal shape of aerostat with minimized wind drift and generation of additional lifting force in windy weather (cf. function $S(x/L)$ in Fig. 3b). Let us now keep the geometrical similarity of this shape and apply the procedure of scaling up the aerostat size determined by its total length L. Then, let us define the quantity $R_v = \beta_v L$ as the radius of the roller with the same length L and the same volume of our aerostat. Analogously, let us define the quantity $R_s = \beta_s L$ as the radius of roller with the same length L and the same lateral surface of our aerostat. One can express the design volume V_0 and the design lateral surface S_0 for the configuration of the model at the starting point (at the initial level H_1, pressure difference $\Delta p = 0$ and temperature $T = T_1$) as follows:

$$V_0 = \pi (R_v)^2 L = \pi (\beta_v)^2 L^3 \tag{1}$$

$$S_0 = 2\pi R_s L = 2\pi \beta_s L^2 \tag{2}$$

By assuming the scaling process based on geometrical shape similarity rule and the scaling coefficient α as well as general dependence of aerostat volume on pressure and temperature expressed by coefficient k_v, one obtains the formula for the volume and lateral surface of the scaled aerostat:

$$V_\alpha(\Delta p, \Delta T) = \pi (\beta_v)^2 (\alpha L)^3 k_v(\Delta p, \Delta T) \tag{3}$$

$$S_\alpha(\Delta p, \Delta T) = 2\pi\beta_s(\alpha L)^2 k_s(\Delta p, \Delta T) \tag{4}$$

where $k_v(\Delta p, \Delta T)$, $k_s(\Delta p, \Delta T)$ are the coefficients describing the change of aerostat volume and surface, respectively, depending on gas overpressure inside the aerostat Δp and temperature change ΔT in relation to the initial temperature T_1. In the simplest case, the coefficient k_v depends linearly on gas overpressure Δp according to the formula:

$$k_v(\Delta p, \Delta T) = k_v(\Delta p) = 1 + k^{-1}\Delta p \tag{5}$$

where k is the constant determined from experimental or numerical analysis.

The total mass of the scaled aerostat can be calculated using initial lateral surface of the aerostat, its initial volume and mass of payload as:

$$M = S_\alpha(0, 0)\delta_s + V_\alpha(0, 0)(\delta_h + \delta_v) + M_p \tag{6}$$

where: δ_s—specific mass of the aerostat surface at the initial altitude H_1, δ_h, δ_v, respectively, density of helium and internal structure (per unit volume, including the mass of ballonets and air in one of them) at the initial altitude H_1 and M_p—mass of the payload to be carried up. In the consequence, the force acting on the aerostat F_α, being the difference of aerostat weight and the buoyancy force at a given altitude H, can be expressed as follows:

$$F_\alpha(\Delta p, \Delta T) = Mg(H) - V_\alpha(\Delta p, \Delta T)\delta_a(H)g(H) \tag{7}$$

where: $\delta_a(H)$—specific mass of air at the altitude H. The optimal scaling up of the CANDY aerostat in order to design Aero-SDT for the planned mission to be performed (between H_1 and H_2 and for the payload M_p) leads to determination of minimum value of scaling coefficient α for which the force acting on the aerostat is negative $F_\alpha \leq 0$.

5 The Case Studies

5.1 Numerical Model

The two numerical models of the mini-aerostat (CANDY) were prepared using Abaqus software. In the first variant, a tight, non-stretchable nylon fabric partially coating a flexible aerostat membrane was applied in order to limit deformations caused by internal pressure (Fig. 6a). For comparison, the alternative model which does not contain any constraints was developed (Fig. 6b). In both cases, the aerostat models were suspended on the cable. The designed mini-aerostat is 3.06 m long and has 0.78 m in diameter. It is made of polyurethane film weighing 1.600 kg, whereas

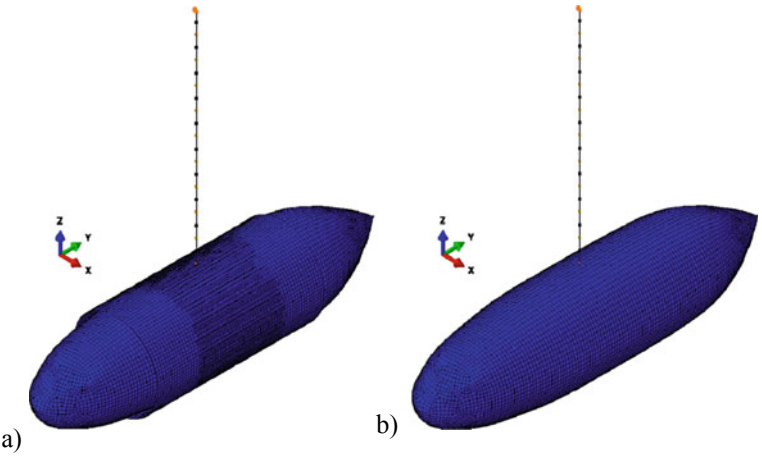

Fig. 6 Two numerical models of the suspended aerostat: **a** with constraints—non-stretchable fabric and **b** without constraints

the nylon fabric weighs 0.228 kg. The total mass of the aerostat is equal to 2.955 kg. The aerostat contains three chambers: the rear air-filled ballonet (0.098 m^3), the front air-filled ballonet (0.100 m^3) and helium-filled main chamber (0.807 m^3).

Numerical computations are based on membrane finite elements used for aerostat membrane and ballonets (11 112 elements) and for nylon fabric (5 820 elements). The rope (10 elements) is fixed at the upper end and another end is connected to the nylon fabric (Fig. 6a) or to the aerostat membrane (Fig. 6b). Changes of mass of gas in all chambers are controlled by inflators, defined for each chamber.

Independently, for comparison purposes, an experimental test was performed. In the initial configuration of the aerostat, the both ballonets were empty, whereas main chamber was filled with helium with zero overpressure. Next, some amount mass of helium was inflated into the main chamber resulting in overpressure, and then a portion of air was pumped into the front ballonet. The rear ballonet remained all the time uninflated.

The volume changes were recorded by the optic measuring technique discussed in Sect. 3. Additionally, pressure sensors were located in the front ballonet and the main chamber. The tensile force data in the suspension cable was collected by a force sensor. Obtained results of the numerical computation and the experimental test were summarized in Table 1.

The measured results given in Table 1 are coinciding with numerical simulation. In the next step, the scaling procedure presented in Sect. 4 is applied in Sect. 5.2.

Table 1 Results of numerical computation and experimental results

State	Total volume		Pressure		Force
	Measured (optic) [m^3]	Computed [m^3]	Measured [Pa]	Computed [Pa]	Measured [N]
Initial configuration	1.0102	1.0049	0.0	0.0	16.90
Main chamber inflation (helium)	1.0663	1.0548	Main chamber: 953	Main chamber: 947	16.36
Front ballonet inflation (air)	1.0697	1.0582	Main chamber: N/A	Main chamber: 1025	16.50
			Front ballonet: 830	Front ballonet: 1026	

5.2 Numerical Simulation of Aero-SDT Mission

Data obtained from experimental measurements can be used to build a numerical model of vertical motion of the CANDY demonstrator. Based on the identified model parameters and the scaling assumptions presented in the previous sections, sample analyses of the operational capabilities of the scaled aerostats were performed. Selected results are summarized in Table 2. During the simulation, a mission was assumed to lift a 0.5 kg payload to the maximum height that can be achieved with a given type of scaled structure.

The presented results show that both the initial structure and the structure with lengths scaled by the $\alpha = 1.7$ factor do not have the ability to ascend at the assumed density parameters of the materials used. Only the scaled structures with α value greater than 1.7 allow the aerostat to realize the mission.

Figure 7 shows the results of the aerostat mission for the scale factor of $\alpha = 1.8$. The left chart presents the exemplary altitude changes in time. One can see the maximum operating altitude which is just over 500 m. On the other hand, in Fig. 7b, the variation of the buoyancy force and the total weight as a function of time are shown. During the initial phase of movement, it is visible that the buoyancy force is greater than the weight causing the aerostat to ascend to its maximum height. This operation is accompanied by drop of the buoyancy force. Despite the decrease in atmospheric pressure, the coating material above a certain volume must be stretched which limits the change in volume. The aerostat maintains altitude when it is in equilibrium. Then, after releasing a small amount of helium, the buoyancy force is smaller than the weight, which causes the aerostat to descend. It is worth noting that as the altitude decreases, the atmospheric pressure increases which additionally decreases the volume and buoyancy force.

Table 2 Results of numerical simulations of aero-SDT mission

α	V/V_o	L	D	V	A	Specific mass δ_v	Specific mass δ_s	k	Payload	Buoyancy force (initial)	Weight	Maximal altitude
1.0	1.0	3.06	0.79	1.01	6.14	0.30	0.20	18,868	0.50	12.45	21.70	0.00
1.7	4.9	5.20	1.35	4.94	17.76	0.30	0.20	6739	0.50	60.90	62.75	0.00
1.8	5.8	9.36	2.42	5.86	19.91	0.30	0.20	5896	0.50	72.35	71.27	520.00
2.0	8.0	6.12	1.58	8.04	24.58	0.30	0.20	3494	0.50	99.30	90.55	1760.00

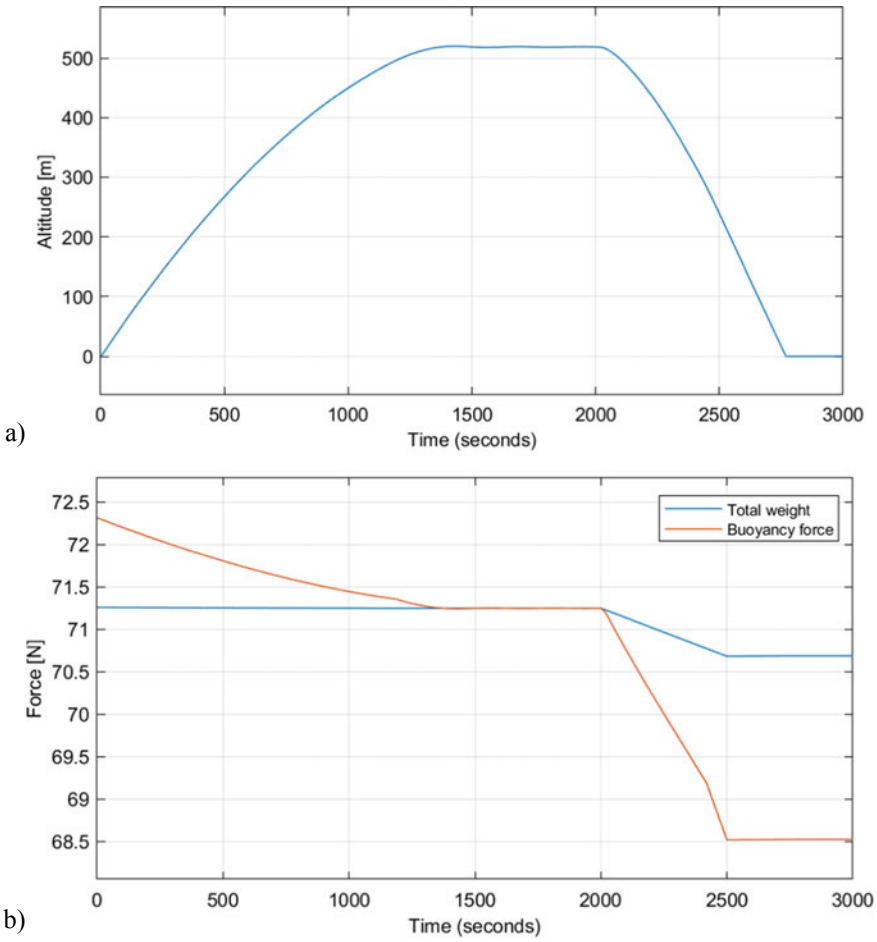

Fig. 7 Simulation results of the mission for the aerostat scaled by $\alpha = 1.8$: **a** altitude changes and **b** changes in buoyancy force and aerostat weight

6 Discussion and Conclusions

The important limitations of aerostats design (especially their ability to carry required payloads or to achieve assumed altitudes) are the problems related to selection of appropriate aerostat internal structure and volume affecting the necessary lift force. A significant change in payload or target altitude causes the requirement of resizing the aerostat. Although it is possible to use oversized aerostats, operating them is associated with higher costs (e.g. the need to use much larger mass of expensive gases or increased fuel consumption). For this reason, we address the novel concept of designing the customized aerostat based on a mini-models (CANDY) which can be more easily verified and tested. If such a design is properly functioning, the

dedicated scaling procedure for aerostats dimensions can be applied. We also present preliminary results of numerical tests of a proposed design. The final validation of the proposed procedure of designing helium-filled aerostats and mini-models CANDY and the scaling procedure will be experimental fly testing in near real conditions using SKYLAB.

Acknowledgements The authors acknowledge the support of the National Centre for Research and Development and the National Science Centre, Poland, granted in the framework of the TANGO 4 programme (project TANGO-IV-C/0001/2019-00).

References

1. Recent Development Efforts for Military Airships, The Congress of the United States, Congressional Budget Office (CBO), November 2011, https://fas.org/irp/program/collect/cbo-airship.pdf
2. Saleh S, Weiliang HE (2018) New design simulation for a high-altitude dual-balloon system to extend lifetime and improve floating performance. Chin J Aeronaut 31(5):1109–1111
3. Loon.com. The Stratosphere: High Altitude, Higher Ambitions, https://loon.com/resources/content-library. Accessed on June 21 2021
4. Ghanmi A, Sokri A (2010) Airships for military logistics heavy lift. Defence R&D Canada, Centre for Operational Research and Analysis, DRDC CORA TM 2010-011, 2010, https://cradpdf.drdc-rddc.gc.ca/PDFS/unc92/p532881.pdf
5. Future Aerostat and Airship Investment Decisions Drive Oversight and Coordination Needs (2012) Report to the Subcommittee on Emerging Threats and Capabilities, Committee on Armed Services, U.S. Senate, GAO
6. Holnicki-Szulc J, Świercz A, Kostro S, Knap L, Graczykowski C (2021) A concept of the SDT (self-deployable tensegrity) structure for the rapid and precise lifting of helium aerostats, especially into the stratosphere, Patent No. 3770352, EPO
7. Knap L, Świercz A, Graczykowski C, Holnicki-Szulc J (2021) Self-deployable tensegrity structures for adaptive morphing of helium-filled aerostats. Arch Civ Mech Eng 21(159):1–18. ISSN: 1644-9665. https://doi.org/10.1007/s43452-021-00292-6